EVALUATION OF THE RELIABILITY OF A FLAWED PIPE

N. CONSTANTIN, D.M. CONSTANTINESCU and St. PASTRAMA

University "Politehnica" of Bucharest
Strength of Materials Department
Splaiul Independentei 313, R-77206, Bucuresti 16, Romania

ABSTRACT

The present study was intended primarily to establish the reliability of a batch of pipes having an inner axial flaw and being subjected to an internal pressure. The influence of the flaw depth on the risk of failure was evaluated. Subsequently, a generalization of the relations obtained was done for a larger size range. First, a FE model was used to obtain the stress concentration factor at the tip of the flaw, for different depths and pipe dimensions. The basic results were very close to those obtained by the BE method. Then, a fracture mechanics approach was considered in order to evaluate the stress intensity factor at the tip of the flaw. In all cases, linear elastic behavior of the material was considered.

KEYWORDS

reliability, flaw, pipe, FE method, BE method, stress intensity factor, J integral, VCE

INTRODUCTION

The aim of this study was primarily to investigate the reliability of a batch of pipes ϕ32x4, having an axial inner flaw, produced in the rolling process. Working in rather heavy conditions of pressure and temperature, it was essential to know the influence of the various depths on the local state of stresses.

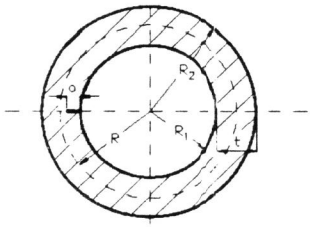

Fig 1 General geometric configuration of the studied problem.

The geometry of the flaw was considered that of Fig. 1, with a 20μm radius at the tip. The magnitude of a was estimated, with adequate ultrasonic equipment to be between 120μm and 200μm, so the flaw could be hardly considered as a typical crack. Consequently, the problem was first solved as a stress concentration problem and then the fracture mechanics aspects were considered.

STRESS CONCENTRATION PROBLEM

In order to investigate the stress concentration around the flaw, two models were considered.

The study was done first with FE model of the pipe section, shown in Fig. 2, taking R_1 =12 mm and R_2 =16 mm. The symmetry about one axis was considered and the mesh was progressively refined towards the flaw. Conventional quadrilateral isoparametric elements were used, under plane strain conditions. The mesh was slightly modified for different depths of the flaw. As Guydish and Fleming (1978) have shown, different meshes can lead to different results when usual elements are used in fracture mechanics problems. In order to have a control over them, two different meshes were used for one depth of the flaw (a=140μm). The results were slightly different in groups 1 and 2 of elements (see Fig. 2) and identical in groups 3 and 4.

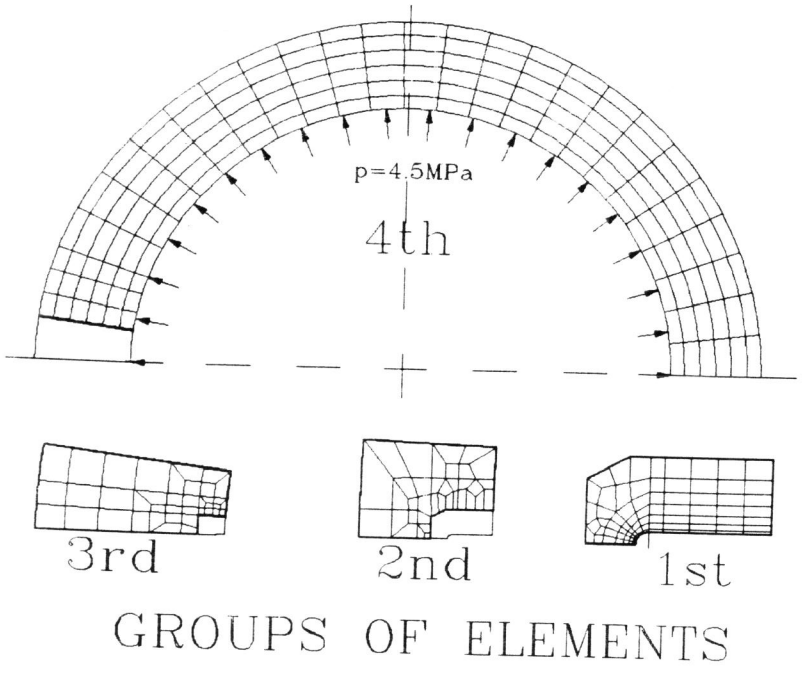

Fig. 2 FE model of the flawed pipe.

The unique loading was an internal pressure of 4.5 MPa(45 bar), which was applied also on the inside of the flaw. the difference between the numerical hoop stresses and the exact ones calculated with the thick-walled theory did not exceed 2.6% for the elements of group 4 in any of the FE model variants. Thermal conditions were taken into consideration by referring to the yield point of the material at the working temperature. In this way, the critical situation was considered to be attained when this value was exceeded by the equivalent normal stress, obtained with the Huber-Hencky-Mises criterion of plasticity:

$$\sigma_{eq} = \sqrt{\frac{1}{2}\left[(\sigma_1-\sigma_2)^2+(\sigma_2-\sigma_3)^2+(\sigma_3-\sigma_1)^2\right]} \qquad (1)$$

where σ_1, σ_2, σ_3 are the principal normal stresses.

Following this idea, a linear relation was obtained between σ^n_{eq} and a, by the least squares method, starting from pairs of values obtained on the FE model. This relation, with a high factor of correlation (0.983), was:

$$\sigma^n_{eq} = 0.297a + 69.5 \qquad (2)$$

and is presented in Fig. 3.

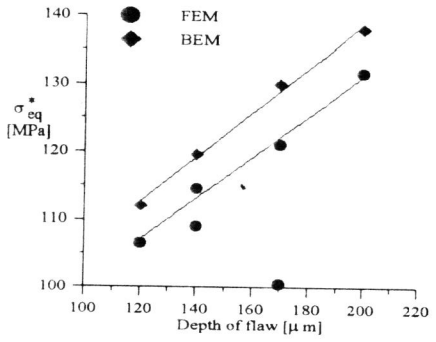

Fig.3 The relation between σ^n_{eq} and depth of flaw obtained by FEM, respectively BEM.

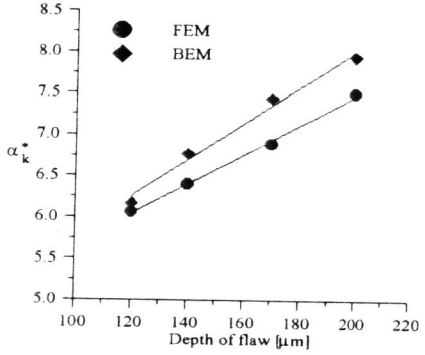

Fig.4 The relation between α^*_k and depth of flaw, obtained by FEM, respectively BEM

For a=140μm, the slightly different value of σ^n_{eq} can be noticed, both being considered to have equal weight in the method. The very low value for a=200 μm was obtained for a different numbering of the nodes (starting from the opposite-to the flaw end of the model). This value was not taken into consideration. As the yield point at the work temperature was 120 MPa, the critical depth of the flaw appeared to be 170 μm.

A similar approach was done using the BE method. For this second model, the nodes defining the elements were chosen in the same portions as those used in the FE method, on the contour of the model.

The values of σ^n_{eq}, for different depths of the flaw, are presented in Fig. 3. The linear relation between σ^n_{eq} and a, obtained in a similar way as before, was

$$\sigma^n_{eq} = 0.34a + 71.2 \qquad (3)$$

and is presented in Fig. 3. All this data were obtained under the same plane strain assumptions, as in the FE model. This time, it can be seen that the critical depth of the flaw was 144μm.

The analysis of the flaw effect on the stress distribution in the pipe was generalized, using only the FE method. A stress concentration factor α_k* at the tip of the flaw was defined as:

$$\alpha_k^* = \frac{\sigma_{eq}^n}{\sigma_{eq}^a} \tag{4}$$

where σ_{eq}^n was the equivalent normal stress obtained with the FE model and σ_{eq}^a, the similar stress with the thick-walled tubes theory. For both values, formula (1) was used, in which the principal stresses were numerically obtained in the first case, and, in the second case, were calculated as follows:

$$\sigma_1 = p\frac{R_1^2}{R_2^2 - R_1^2}\left(1 + \frac{R_2^2}{r^2}\right)$$
$$\sigma_2 = \nu(\sigma_1 + \sigma_3) \tag{5}$$
$$\sigma_3 = p\frac{R_1^2}{R_2^2 - R_1^2}\left(1 - \frac{R_2^2}{r^2}\right)$$

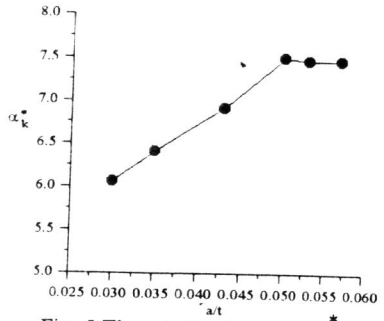

Fig. 5 The relation between α_k^* and a/t obtained by FEM.

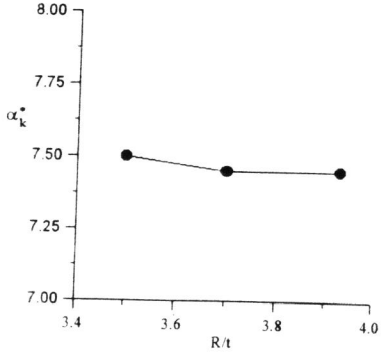

Fig. 6 The relation between α_k^* and R/t obtained by FEM.

In this way, σ_{eq}^a was calculated with the nominal normal stresses at the tip, located at the radius r = R_1+a. The Poison's ratio was considered to be 0.3.

In Fig. 5 are presented the values for α_k^* for the values of a considered before, obtained by FEM and BEM respectively. In Fig. 5 and 6 are presented the relations between α_k^* and a/t and R/t respectively, when supplementary values for R_1, R_2,and a were considered. In Fig. 7 is presented the evolution of α_k^* at the tip, in the bulk material in the plane of the flaw.

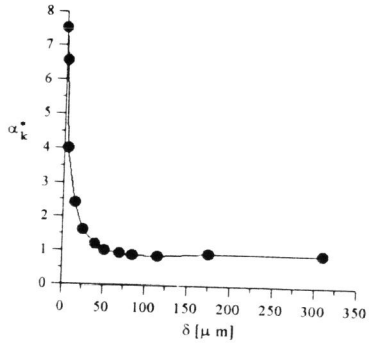

Fig. 7 Evolution of α_k^*, at the tip of the flaw, obtained by FEM.

FRACTURE MECHANICS PROBLEM

A fracture mechanics approach was also considered in order to evaluate the stress intensity factor at the tip of the flaw.

First, a theoretical evaluation was done, using the relations found in Anderson(1991) for the calculation of the stress intensity factor for mode I; in the case of a long part-through axial internal flaw in a pipe with internal pressure:

$$K_I = \frac{2pR_2^2}{R_2^2 - R_1^2}\sqrt{\pi a}\cdot F\left(\frac{a}{t}, \frac{R_1}{t}\right) \tag{6}$$

where the function F is given by:

$$F = 1.1 + A\left[4.951\left(\frac{a}{t}\right)^2 + 1.092\left(\frac{a}{t}\right)^4\right] \tag{7}$$

and the coefficient A is:

$$A = \left(0.125\frac{R_1}{t} - 0.25\right)^{0.25} \tag{8}$$

The above formulae are valid for $a/t \le 0.75$ and $5 \le R/t \le 10$. The first condition was fulfilled in all cases, while the ratio R/t was situated between 3.5 and 3.93.

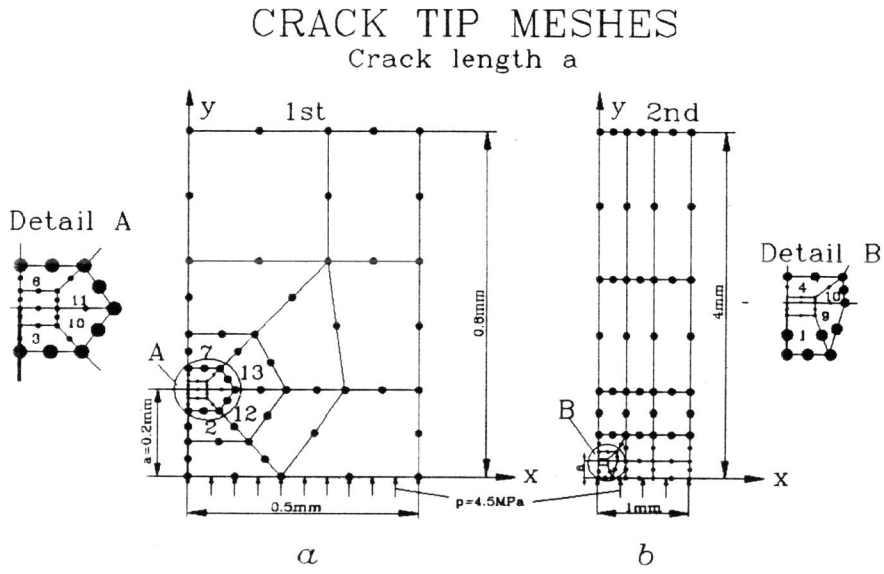

Fig. 8 Fracture mechanics FE model

For example, $K_I = 0.573$ MPa$\sqrt{m}$ in the case when $R_1 = 12$ mm, $R_2 = 16$ mm, $a = 0.2$ mm, t = 4 mm. Anyhow, the values obtained with these formulae were smaller than those found from the numerical modeling.

Numerical values were also obtained, using a special linear-elastic bidimensional FE program. The stress intensity factor was obtained only for the pipe having R_1=12 mm, R_2=16 mm and a=200μm. Two methods were used in order to establish the value of the stress intensity factor: the virtual crack extension (VCE) method and the J-integral. Due to symmetry considerations only half of the region that surrounds the crack was modeled. and this time, quadratic isoparametric elements with eight nodes were used, avoiding the special crack tip singularity elements. The first mesh, mesh 1 (see Fig. 8a), covered only a very small area around the crack tip, having 0.5 mm-width and 0.8 mm depth. The second mesh, mesh 2 (see Fig. 8b), had a width of 1 mm and a depth equal to the thickness of the pipe wall, that is 4 mm.

The VCE was 0.001 for both meshes . The J-integral was calculated as passing through the elements 3-10-11-6 and 2-12-13-7 for mesh 1, and through the elements 1-9-10-4 for mesh 2. It was preferred to employ a 2x2 numerical integration rule since it was shown also by Owen and Fawkes(1983) that the two-point quadrature positions are the optimum location for stress evaluation for the eight-node elements. For the chosen elements, the values of the stress intensity factors were calculated with the J-integral for the paths going through the Gauss points closer to the crack tip, line 1, and farther away, line 2. The obtained results are presented in table 1.

Table 1. Numerical results for the stress intensity factor.

Mesh	*Method*	*Elements*	*J-integral path*	K_I, *[MPa√m]*
Mesh 1	VCE			1.25
	J-integral	3-10-11-6	line 1	1.03
			line 2	1.33
		2-12-13-7	line 1	1.63
			line 2	2.10
Mesh 2	VCE			2.42
	J-integral	1-9-10-4	line 1	1.54
			line 2	2.39

CONCLUSIONS

The study revealed interesting relations in which σ^n_{eq} and mostly α^*_k are involved. For example, the values obtained for σ^n_{eq} were only slightly different when two meshes were used, but very different when renumbering the same mesh. Another interesting aspect was that α^*_k is constant for a small variation of a/t or R/t. It must be mentioned that these narrow intervals for a/t and R/t were obtained by modifying only R_2.

It in also to be noted that α^*_k is very steeply decreasing with the increase of the distance from the tip of the flaw, and attains values slightly under 1 up to a distance of the same order of magnitude as a, before increasing back to 1. Consequently, refining the mesh seems to be essential, at least for the study of the stress concentration factor.

For the fracture mechanics approach, the analytical formulae cannot be used in our problem, and we have to rely on the numerical results. The stress intensity factor calculated by the J-integral is smaller for the elements closer to the crack tip due to the fact that the elements are unable to model the singular behavior near the crack tip. It can be noticed that for the second mesh, which models the entire thickness of the pipe, the stress intensity factor is greater than the one obtained from the first mesh, a fact that seems to be peculiar. The influence of the mesh refinement on the correct value of the stress intensity factor is not yet well understood.

REFERENCES

Anderson, T.L., (1991), Fracture Mechanics - Fundamentals and Applications, CRC Press, Inc., Boca Raton.

Guydish, J.J., Fleming J.F., (1978), Optimization of the Finite Element Mesh for the Solution of Fracture Problems, Engineering Fracture Mechanics, Vol. 10, No. 1, pp. 31-42.

Owen, D.R.J., Fawkes, A.J., (1983), Engineering Fracture Mechanics - Numerical Methods and Applications, Pineridge Press , Ltd., Swansea.